Annals of Hepatology 29 (2024) 101532

Contents lists available at ScienceDirect

Annals of Hepatology

journal homepage: www.elsevier.es/annalsofhepatology

Original article

A novel role of AIM2 inflammasome-mediated pyroptosis in radiofrequency ablation of hepatocellular carcinoma

Feifan He[a,*], Zhongming He[b], Caoye Wang[b,*]

[a] The Fourth Clinical Medical College, Nanjing Medical University, No. 138 Hanzhong Road, Nanjing, Jiangsu Province, China
[b] Interventional Radiology Department, Third Affiliated Hospital of Suzhou University, No. 185 Juqian Road, Changhzou, Jiangsu Province, China

ARTICLE INFO

Article History:
Received 28 February 2024
Accepted 5 June 2024
Available online 22 July 2024

Keywords:
Inflammasomes
Cell death
Liver neoplasms
Caspases
Therapeutics

ABSTRACT

Introduction and Objectives: The absence of melanoma 2 (AIM2) protein triggers the activation of the inflammasome cascade. It is unclear whether AIM2 plays a role in hepatocellular carcinoma (HCC) and radiofrequency ablation (RFA), which uses radiofrequency waves to treat tumors. In this study, we investigated if RFA could induce pyroptosis, also called cell inflammatory necrosis, in HCC through AIM2-inflammasome signaling *in vivo* and *in vitro*.

Materials and Methods: BALB/c nude mice were used to generate HepG2 or SMMC-7721 cell-derived tumor xenografts. HCC cells with knockdown or overexpression of AIM2 were created using short hairpin RNA (shRNA) and expression vector transfection, respectively, for functional and mechanistic studies. Downstream effects were examined using flow cytometry, qRT-PCR, ELISAs, and other molecular assays.

Results: RFA significantly suppressed tumor growth in HCC cell xenografts. Flow cytometry analysis revealed that RFA could induce pyroptosis. Furthermore, AIM2, NLRP3, caspase-1, γ-H2AX, and DNA-PKc had significantly greater expression levels in liver tissues from mice treated with RFA compared with those of the controls. Additionally, interleukin (IL)-1β and IL-18 expression levels were significantly higher in the HCC cell-derived xenograft mice treated with RFA compared with those without RFA. Notably, a significantly greater effect was achieved in the RFA complete ablation group versus the partial ablation group. Knockdown or overexpression of AIM2 in HCC cells demonstrated that AIM2 exerted a role in RFA-induced pyroptosis.

Conclusions: RFA can suppress HCC tumor growth by inducing pyroptosis via AIM2. Therefore, therapeutically intervening with AIM2-mediated inflammasome signaling may help improve RFA treatment outcomes for HCC patients.

1. Introduction

Hepatocellular carcinoma (HCC) is one of the most common malignancies and a leading cause of cancer-related deaths globally [1]. According to Global Burden of Disease data, there are approximately 750,000 HCC cases worldwide [2]. In recent years, global HCC incidence and mortality rates have significantly increased [3]. Notably, the majority of HCC cases occur in Asian countries [4]. In China, the HCC incidence is considerably high, accounting for approximately 50% of all newly diagnosed HCC cases across the world, with about 326,000 patients dying each year. This can be attributed to the particularly high prevalence of chronic hepatitis B virus (HBV) infection [4–6]. In fact, HBV and hepatitis C virus (HCV) are common causes of chronic hepatitis and progressively cause inflammation of the liver. Although the exact pathogenic mechanisms underlying HCC remain to be elucidated, hepatic inflammation and inflammasome-mediated molecular mechanisms have

Abbreviations: AIM2, absent in melanoma 2; cGAS, cyclic GMP-AMP synthase; CTNNB1, catenin beta 1; DNA-PKc, DNA-dependent protein kinase catalytic subunit; ELISA, enzyme-linked immunosorbent assay; FAM, fluorescein acetoxymethyl; FLICA, fluorescent-labeled inhibitors of caspase; GAPDH, glyceraldehyde-3-phosphate dehydrogenase; γ-H2AX, gamma H2A histone family member X; HBV, hepatitis B virus; HCC, hepatocellular carcinoma; HCV, hepatitis C virus; H&E, hematoxylin and eosin; IL-1β, interleukin-1β; IL-18, interleukin-18; LDH, lactate dehydrogenase; mTOR, mechanistic target of rapamycin; NC, negative control; NLRP3, Nod-like receptor pyrin domain-containing 3; qRT-PCR, quantitative reverse transcription-polymerase chain reaction; RFA, radiofrequency ablation; RPMI, Roswell Park Memorial Institute; SD, standard deviation; STING, stimulator of interferon genes; TERT, telomerase reverse transcriptase; TP53, tumor protein P53; VEGF, vascular endothelial growth factor; WNT, Wingless + Int-1

* Corresponding authors.
E-mail addresses: 937139075@139.com (F. He), caoyewang@139.com (C. Wang).

https://doi.org/10.1016/j.aohep.2024.101532

been proposed to play roles in the pathogenesis of HBV- and HCV-related HCC. In addition, HCC is considered an inflammation-related malignancy [7–10]. For example, nonalcoholic steatohepatitis (NASH) is a progressive form of nonalcoholic fatty liver disease that is associated with hepatocyte injury and liver inflammation. NASH is a major risk factor for developing HCC and involves complex immune responses that are not fully clear.

Currently, curative treatments are viable for less than 30% of new HCC patients, and sorafenib is the standard treatment for advanced stages [3]. Of the various treatment methods for HCC, radiofrequency ablation (RFA) has emerged as an effective and safe approach for patients with small-sized tumors, usually 3 cm or less in diameter. Compared with traditional hepatic resection and liver transplantation, RFA has been associated with less invasiveness and a shorter hospital stay. Under the guidance of imaging, one or more thin needles are inserted through the skin into the tumor. A RF current is then established, which generates a high temperature and leads to tumor cell necrosis [11]. Despite the advantages and increasing application of RFA for treating HCC, the molecular details underlying its specific mechanism of action are not well understood.

Recent advances in genomic profiling have identified frequent mutations in genes such as *telomerase reverse transcriptase* (*TERT*), *catenin beta 1* (*CTNNB1*), and *tumor protein P53* (*TP53*), which help to classify HCC molecular subtypes [3]. These genomic discoveries have enabled new clinical therapies targeting specific genetic alterations through preclinical validation models, including genetically engineered mice and xenograft models, as well as various HCC cell lines. Pathway analyses have shown that Wingless + Int-1 (WNT)/β-catenin, vascular endothelial growth factor (VEGF), and mechanistic target of rapamycin (mTOR) are critical for HCC progression, facilitating the development of agents including sorafenib, regorafenib, and lenvatinib [3].

Absent in melanoma 2 (AIM2) is a cytosolic receptor in the pyrin and hematopoietic expression, interferon-inducible nature, and nuclear localization (HIN) domain-containing protein family [12,13]. AIM2 can sense and bind to both double-stranded DNA and apoptosis-associated speck-like protein, thus triggering activation of the inflammasome signaling cascade and assembly of the AIM2 inflammasome [14–16]. Activation of the AIM2 inflammasome, which consists of multiple proteins, represents a key aspect of inflammation pathways. The AIM2 inflammasome can activate caspase-1, leading to the induction, maturation, and release of key pro-inflammatory cytokines, such as interleukin (IL)-1β and IL-18 [17]. Therefore, the AIM2 inflammasome possesses both pro-inflammatory and pro-pyroptotic properties to mediate pyroptosis, a type of programmed cell death that is also known as cell inflammatory necrosis. During this process, the cells continue to expand until the cell membrane bursts, which results in cellular content release and activation of a strong inflammatory response.

Pyroptosis has been implicated in host defense mechanisms, thus combating microbial invasion, carcinogenesis, and cancer progression. Several previous studies have reported that AIM2 expression levels are decreased in HCC tissues compared with histologically normal tissues [18,19]. Additionally, lower AIM2 expression levels are significantly correlated with more advanced HCC [20,21]. Currently, how AIM2 is involved in HCC remains largely unknown. In addition, whether AIM2 exerts a role in the RFA mechanism of action in HCC has not yet been explored.

In the present study, we aimed to investigate the roles of AIM2 in HCC and explore the use of RFA for treating this disease. *In vitro* experiments with hepatoma cells and *in vivo* work with a xenograft tumor mouse model were conducted. Our results suggested that AIM2-mediated activation of inflammasome signaling is an important cell death mechanism in HCC. Lower AIM2 levels are significantly correlated with more advanced HCC cases. The findings obtained in this study may offer a better understanding of the biological function of AIM2, the AIM2 inflammasome, and pyroptosis in HCC, thereby potentially helping to improve RFA-based treatment methods for HCC. This investigation may also support more effective and personalized treatment strategies for HCC.

2. Materials and Methods

2.1. Cell culture

Two human HCC cell lines, HepG2 and SMMC-7721, were obtained from Shanghai Binsui Biotechnology (Shanghai, China) and used for the *in vitro* studies. The HepG2 and SMMC-7721 cells were cultured in Roswell Park Memorial Institute (RPMI) 1640 medium (Hyclone, Marlborough, MA, USA) supplemented with 10% fetal bovine serum (FBS), 100 μg/mL streptomycin, and 100 units/mL penicillin. Cells were incubated at 37°C and 5% CO_2.

2.2. Experimental animals

BALB/c nude mice (4–6 weeks old) were purchased from Jiangsu Synthgene Biotechnology Co., Ltd. (Nanjing, Jiangsu, China). The mice were housed under controlled conditions and given access to tap water ad libitum throughout the experimental period. To establish the HepG2 and SMMC-7721 cell-derived tumor xenograft animal models, BALB/c nude mice were subcutaneously injected with HepG2 cells (1×10^7 cells suspended in 100 μL of serum-free medium) or SMMC-7721 cells (1×10^7 cells suspended in 100 μL of serum-free medium). HepG2 or SMMC-7721 cell-derived xenograft nude mice were randomly assigned to receive RFA complete ablation (no remaining tumor), RFA partial ablation (some tumor remaining), or no ablation as a control (non-ablation). Blood samples were taken from the mice via the jugular vein, then were centrifuged at 1,110 $\times$ g for five minutes to separate the serum. Four weeks following the treatment, the mice were anesthetized and sacrificed by cervical dislocation, then the tumors were collected. The weights and volumes of the excised tumors were analyzed.

The study involving experimental mice was reviewed and approved by the Ethics Committee of Changzhou First People's Hospital (Approval No. 2018-025). All methods were carried out in accordance with the local institutional and national guidelines and regulations. In addition, the experiments were performed in compliance with the international regulations for the use of laboratory animals.

2.3. RFA

HepG2 or SMMC-7721 cell-derived xenograft nude mice were treated with RFA using a Cool-tip^{TM} RFA Electrode kit (Covidien IIc, Mansfield, MA, USA) according to the manufacturer's protocol. For the *in vitro* study, RFA was performed using a thermal needle to treat SMMC-7721 cells.

2.4. Histology

Tumor tissues from the HepG2 and SMMC-7721 cell-derived xenograft nude mice were formalin fixed, paraffin-embedded (FFPE), then cut into 2-μm sections. After staining with hematoxylin and eosin (H&E), the slides were examined by light microscopy.

2.5. Immunohistochemistry (IHC)

IHC analysis was performed to assess the protein expression levels of AIM2, Nod-like receptor pyrin domain-containing 3 (NLRP3), and caspase-1 in the liver tissues from HepG2 and SMMC-7721 cell-derived xenograft nude mice treated with or without RFA. The liver tissues were processed into FFPE blocks. These FFPE liver tissue samples were sectioned and hydrated, then incubated with primary

antibodies (1:1000 for all), including those targeting AIM2 (Abcam, Cambridge, UK, ab204995), NLRP3 (Abcam, ab263899), and caspase-1 (Abcam, ab207802), at 4°C overnight. The sections were then incubated with horseradish peroxidase (HRP)-conjugated secondary antibodies at 37°C for 30 minutes. The slides were incubated with 3,3′-diaminobenzidine (DAB), a substrate for HRP, using a DAB Peroxidase Substrate kit according to the manufacturer's instructions (Vector Laboratories, Burlingame, CA, USA). Images were taken using an Olympus digital electron microscope (Olympus, Tokyo, Japan). The immunoreactivities of the IHC images were evaluated for each slide.

2.6. Overexpression of AIM2

The pcDNA 3.1 vector was used to construct the expression vector (OS-AIM2) by inserting the AIM2-encoding cDNA sequence. The successful construction of OS-AIM2 was verified by sequencing. SMMC-7721 cells were transfected with OS-AIM2 for overexpression of AIM2 using Lipofectamine 2000 Reagent (Invitrogen, Carlsbad, CA, USA).

2.7. Knockdown of AIM2

AIM2 was knocked down using short hairpin RNAs (shRNAs). Two shRNAs were designed to target AIM2 (AIM2-shRNA1 and AIM2-shRNA2). A scramble shRNA was used as a negative control. The specific sequences were as follows: AIM2-shRNA1, forward: 5′-CCGGCAGCCATCAGAAATGATGTCGCAAACTCGAGGAATTTTGCGA-CATCATTTCTGATGGCTGTTTTTG-3′, reverse: 5′-AATTCAAAAACAGC-CATCAGAAATGATGTCGCAAAATTCCTCGAGTTTGCGACATCATTTCT-GATGGCTG-3′; AIM2-shRNA2, forward: 5′-CCGGGAGATAA GGTTCGACTTACATTCTTCTCGAGAAGAATGTAAGTCGAACCTTATCTCT TTTTG-3′, reverse: 5′-AATTCAAAAAGAGATAAGGTTCGACTTA-CATTCTTCTCGAGAAGAATGTAAGTCGAACCTTATCTC-3′; scramble, forward: 5′-CCGGAACAGTCGCGTTTGCGACTGGCTCGAGCCAGTCG-CAAACGCGACTGTTTTTTTG-3′, reverse: 5′-AATTCAAAAAAA-CAGTCGCGTTTGCGACTGGCTCGAGCCAGTCGCAAACGCGACTGTT-3′. SMMC-7721 cells were transfected with shRNAs using Lipofectamine 2000 Reagent.

2.8. Lactate dehydrogenase (LDH) release assay

Cellular damage and proliferation were measured using an LDH release assay. LDH is a cytosolic enzyme that is released into the culture medium upon cell membrane damage, making it a useful marker for evaluating cell viability and cell death [22]. LDH can also be used as a marker of cell proliferation owing to its role in the metabolic processes of rapidly dividing cells [23]. In this study, SMMC-7721 cell culture supernatants were examined using an LDH release assay kit (Abcam) according to the manufacturer's instructions. Cells (1×10^5 cells/mL) were seeded in 96-well plates for these assays, with 100 μL cell suspension per well.

2.9. Flow cytometry analysis of pyroptotic cells

Pyroptosis was measured on a flow cytometer (Becton, Dickinson and Company, Franklin Lakes, NJ, USA). Fluorescent-labeled inhibitors of caspase (FLICA) probe assays (AAT Bioquest, Sunnyvale, CA, USA) were conducted to examine pyroptosis according to the manufacturer's instructions. Pyroptotic cells were specifically stained by fluorescein acetoxymethyl (FAM)-FLICA-caspase-1 and propidium iodide staining.

2.10. Enzyme-linked immunosorbent assays (ELISAs)

ELISAs were performed to determine the serum levels of IL-1β and IL-18 in HepG2 and SMMC-7721 cell-derived xenograft nude mice treated with or without RFA, as well as in the SMMC-7721 cell culture supernatants, following instructions included in the specific Abcam kits. For ELISAs, cells (1×10^5 cells/mL) were seeded in 96-well plates, with 100 μL cell suspension per well.

2.11. Real-time quantitative reverse transcription–polymerase chain reaction (qRT-PCR)

Total RNA was extracted from SMMC-7721 cells using TRIzol (Invitrogen). The total RNA samples were reverse transcribed into cDNA using the Vazyme Biotech (Nanjing, China) reverse transcription kit according to the manufacturer's instructions. Then, qRT-PCR reactions (20 μL) were performed to measure the relative mRNA expression levels of target genes (pyroptosis-related genes) using the 2 × ChamQ Universal SYBR qPCR Master Mix (Vazyme Biotech) and 10 μM of each primer. β-actin expression was used as an internal control. The relative mRNA levels of target genes were obtained by using the $2^{-\Delta\Delta Ct}$ method, with all assays performed in triplicate. Fold-change values were calculated by comparative Ct analysis after normalization to β-actin. The sequences of the primers used in the qRT-PCR analysis were as follows: AIM2, forward primer: 5'-ATCAGGAGGCTGATCCCAAA-3', reverse primer: 5'-TCTGTCAGGCTTAACATGAG-3'; β-actin, forward primer: 5'-GGCACCACACCTTCTACAATG-3', reverse primer: 5'-TAGCACAGCCTGGA-TAGCAAC-3'; NLRP3, forward primer: 5'-AAAGAGATGAGCC-GAAGTGGG-3', reverse primer: 5'-TCAATGCTGTCTTCCTGGCA-3'; caspase-1, forward primer: 5'-CGACAAGGTCCTGAAGGAGA-3', reverse primer: 5'-CCCTTTCGGAATAACGGAGT-3'; gamma H2A histone family member X (γ-H2AX), forward primer: 5'-AGCACTTGGTAACAGGCA-CATCTTC-3', reverse primer: 5'-GTCCACATAGCCAGCCGTGA-3'; DNA-dependent protein kinase catalytic subunit (DNA-PKc), forward primer: 5'-CCAGCTCTCACGCTCTGATATG-3', reverse primer: 5'-CAAACG-CATGCCCAAAGTC-3'; IL-1β, forward primer: ATGATGGCTTATTA-CAGTGGCAA, reverse primer: GTCGGAGATTCGTAGCTGGA; IL-18, forward primer: ATGCTCTGTTTGGGCTGGATA, reverse primer: GTGA-GAGTCGATTTCTGTGGC.

2.12. Western blot analysis

Western blot analysis was performed to examine the hepatic protein levels of AIM2 and key inflammasome- and pyroptosis-related proteins, such as NLRP3 (Abcam, ab263899), caspase-1 (Abcam, ab207802), γ-H2AX (Abcam, ab81299), and DNA-PKc (Thermo Fisher Scientific, 18-2). The protein expression of glyceraldehyde-3-phosphate dehydrogenase (GAPDH) (Abcam, ab9485) was used as a loading control. Briefly, total protein was extracted from 20 mg of tumor tissue using radioimmunoprecipitation assay (RIPA) buffer (Solarbio, Beijing, China) supplemented with 1% protease inhibitor and phosphatase inhibitor. Lysis was performed on ice for 30 minutes, followed by centrifugation at 12,000 × g at 4°C for 10 minutes. The supernatant was collected and protein quantification was performed using a bicinchoninic acid (BCA) protein concentration assay kit (Thermo Fisher Scientific, Waltham, MA, USA) following the manufacturer's instructions.

Next, 30–50 μg of total protein was separated on 4%–15% sodium dodecyl sulfate–polyacrylamide gels. After electrophoretic transfer onto Immun-Blot polyvinylidene difluoride membranes (Biotides Company, Beijing, China), the blots were blocked with phosphate-buffered saline (PBS) containing 5% nonfat dry milk and 0.1% Tween-20, followed by incubation with primary antibody (1:1000 for all) overnight at 4°C. The membranes were then incubated with secondary antibodies (1:10,000) at room temperature for 1 hour. Chemiluminescence development using DAB and H_2O_2 was then performed. A chemiluminescence imaging system (Bio-Rad, Hercules, CA, USA) was used to determine the relative optical density of each specific band.

2.13. Statistical analysis

Statistical analysis was conducted with SPSS software version 16.0 for Windows (SPSS Inc., Chicago, IL, USA). All experiments included at least triplicate samples for each treatment group, and the data are expressed as the mean ± standard deviation (SD). Representative images are presented for the IHC and western blot results. Analysis of variance (ANOVA) was applied to compare the means of multiple groups. $P < 0.05$ indicated a statistically significant difference between groups.

2.14. Ethical statements

The Ethics Committee of [Anonymized for double-blind peer review] approved all animal experiments (Approval No. 2018-25). The study was conducted in compliance with the ARRIVE guidelines to ensure ethical reporting of animal research.

3. Results

3.1. RFA suppressed tumor growth in subcutaneous xenograft nude mice

We initially assessed the effects of RFA on *in vivo* tumor growth in subcutaneous xenograft nude mice. As shown in Fig. 1A/B, HepG2 and SMMC-7721 cell-derived xenograft tumors in the no-RFA control group grew progressively. However, RFA treatment markedly suppressed tumor growth after four weeks of treatment, as demonstrated by the significantly smaller tumor size and lower tumor weight compared with those of the controls. It was also noted that the tumor sizes were significantly smaller and the tumor weights were significantly lower in the HepG2 and SMMC-7721 cell-derived xenograft nude mice treated with complete RFA ablation than in those treated with partial RFA ablation after four weeks of treatment ($P < 0.05$) (Fig. 1A/B). Consistent with these changes, H&E staining of tumor sections revealed a significant reduction in the number of tumor cells in the HepG2 and SMMC-7721 cell-derived xenograft nude mice treated with complete or partial RFA ablation compared with the control mice (Fig. 1C). In addition, flow cytometry analysis showed that the percentages of pyroptotic cells were 12.62%, 10.75%, and 5.49% (HepG2) and 26.42%, 9.84%, and 3.53% (SMMC-7721) in the complete, partial, and no-RFA ablation groups, respectively (Fig. 1D). Statistical analysis indicated that the proportion of pyroptotic tumor cells was significantly increased in the subcutaneous xenograft nude mice treated with RFA partial or complete ablation compared with the no-RFA ablation control group ($P < 0.01$) (Fig. 1D). Moreover, there was a significantly greater effect in the RFA compete ablation group compared with the partial ablation group ($P < 0.01$).

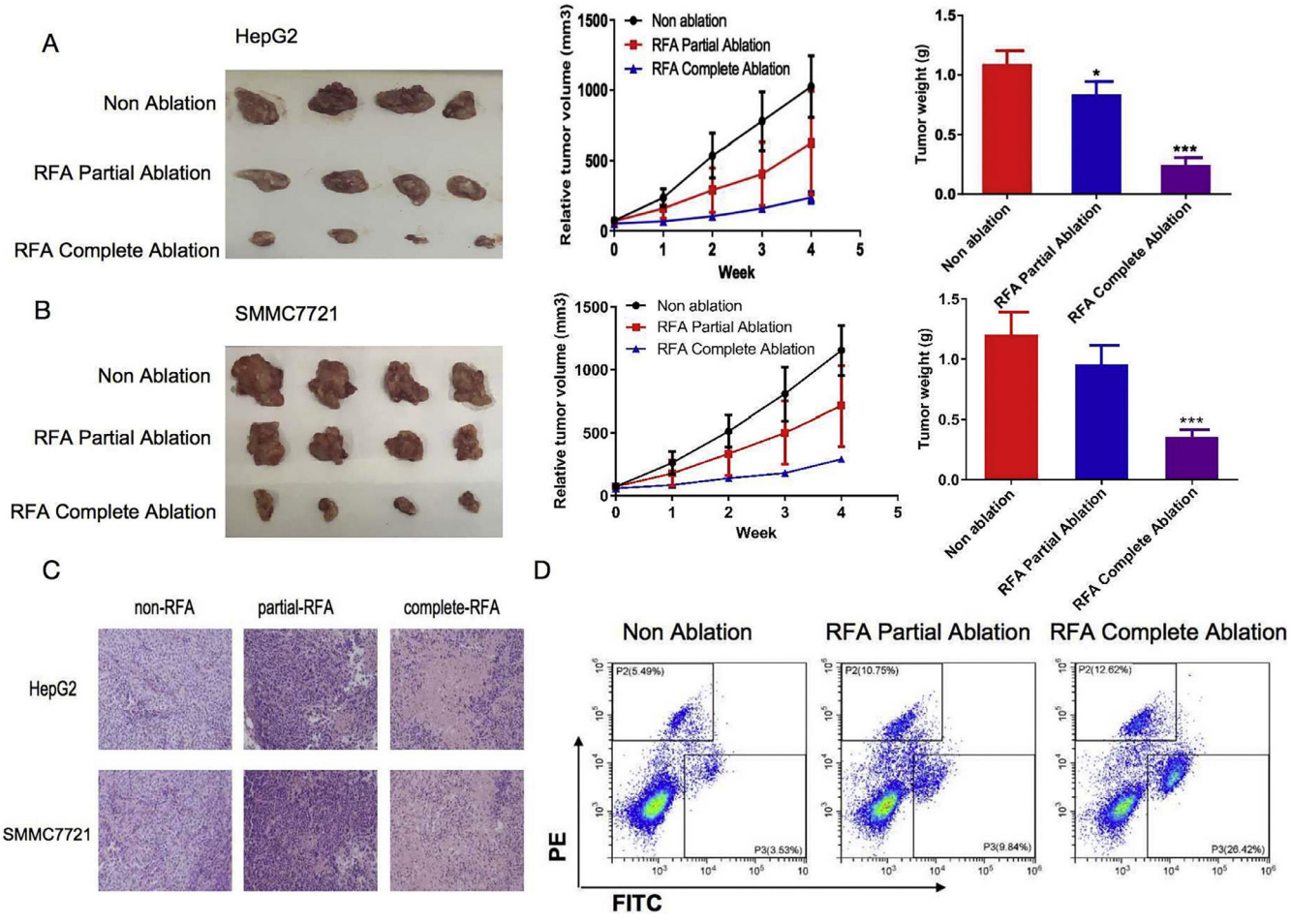

Fig. 1. Inhibitory effects of radiofrequency ablation (RFA) on tumor growth in subcutaneous xenograft nude mice. HepG2 and SMMC-7721 cell-derived xenograft nude mice were used to examine the effects of RFA on tumor growth. The mean tumor sizes and weights were analyzed in the following three groups: No ablation as a control (Non-ablation), RFA partial ablation, and RFA complete ablation. (A) HepG2 cell-derived xenograft nude mice. Tumor growth was significantly suppressed four weeks after RFA partial or complete ablation, as indicated by the smaller tumor size and lower tumor weight compared with the no-RFA treatment control mice. (B) SMMC-7721 cell-derived xenograft nude mice. Tumor growth was significantly suppressed four weeks after RFA complete ablation, as indicated by the smaller tumor size and lower tumor weight compared with the no-RFA treatment control mice. (C) Histological findings of tumor sections from HepG2 and SMMC-7721 cell-derived xenograft nude mice. Hematoxylin and eosin staining of the tumor sections revealed a significant reduction in the number of tumor cells in the HepG2 and SMMC-7721 cell-derived xenograft nude mice treated with complete or partial RFA ablation compared with the control mice. (D) Flow cytometry analysis of pyroptotic cells in subcutaneous xenograft nude mice treated with complete or partial RFA ablation in comparison with the control mice. Data are presented as the mean ± SD. $^{*}P < 0.05$; $^{***}P < 0.001$.

3.2. RFA induced pyroptosis in subcutaneous xenograft nude mice

Given the inhibitory effects of RFA on tumor growth, we next assessed pyroptosis levels in subcutaneous xenograft nude mice at different time points after RFA treatment. IHC and western blot analyses were performed to examine the expression levels of key proteins involved in the inflammasome and pyroptosis in liver tissues from the HepG2 and SMMC-7721 cell-derived xenograft nude mice. The IHC results showed that the AIM2, NLRP3, and caspase-1 protein expression levels were significantly greater in the liver tissue sections of the HepG2 and SMMC-7721 cell-derived xenograft nude mice treated with RFA partial or complete ablation compared with those of the control group ($P < 0.05$) (Fig. 2A/B). In addition, a greater effect of RFA on AIM2, NLRP3, and caspase-1 protein expression was observed in the HepG2 and SMMC-7721 cell-derived xenograft nude mice treated with complete ablation in comparison with partial ablation (Fig. 2A/B). Western blot analysis revealed similar findings to the IHC results. Additionally, the mRNA and protein levels of γ-H2AX and DNA-PKc were significantly greater in the HepG2 and SMMC-7721 cell-derived xenograft nude mice treated with RFA partial or complete ablation versus no-RFA ablation ($P < 0.05$) (Fig. 2C–F). A greater effect was observed in the complete ablation group compared with the partial ablation group (Fig. 2C–F).

The mean levels of serum IL-1β and IL-18 were significantly greater in the HepG2 and SMMC-7721 cell-derived xenograft nude mice treated with RFA partial or complete ablation after four weeks of treatment ($P < 0.05$) (Figs. 3A/B). Notably, there was a greater effect of RFA on IL-1β and IL-18 serum levels in the HepG2 and SMMC-7721 cell-derived xenograft nude mice treated with complete ablation compared with those treated with partial ablation (Fig. 3).

3.3. AIM2 was involved in RFA-induced pyroptosis in hepatoma cells

Intrigued by the animal study findings, we further investigated the biological role of AIM2 in RFA-induced pyroptosis in SMMC-7721 cells *in vitro*. Cell proliferation was evaluated using LDH release assays. The results revealed that shRNA-mediated knockdown of AIM2 enhanced the proliferation of SMMC-7721 cells in a time-dependent manner ($P < 0.05$) (Fig. 4A). In contrast, overexpression of AIM2 using the OS-AIM2 expression vector attenuated the proliferation of SMMC-7721 cells in a time-dependent manner ($P < 0.05$) (Fig. 4B). In addition, exposure to RFA resulted in a marked increase in LDH release compared with no-RFA treatment. Furthermore, overexpression of AIM2 with OS-AIM2 enhanced the LDH release compared with the control SMMC-7721 cells ($P < 0.05$) (Fig. 4C).

Pyroptosis is a form of programmed cell death that can affect tumor cell proliferation. Therefore, we examined the effects of RFA on pyroptosis in hepatoma SMMC-7721 cells with overexpression or knockdown of AIM2. Flow cytometry assays showed that RFA could induce pyroptosis compared with no RFA ($P < 0.05$) (Fig. 5A). Additionally, overexpression of AIM2 with OS-AIM2 enhanced pyroptosis, whereas knockdown of AIM2 with shAIM2 diminished pyroptosis, in SMMC-7721 cells ($P < 0.05$) (Fig. 5A).

Furthermore, qRT-PCR assays revealed that the hepatic γ-H2AX and DNA-PKc mRNA levels were significantly greater in the SMMC-7721 cells treated with RFA versus those not treated with RFA. Moreover, overexpression of AIM2 increased hepatic γ-H2AX and DNA-PKc mRNA expression levels, while AIM2 knockdown led to a decrease in the hepatic γ-H2AX and DNA-PKc mRNA expression levels, in SMMC-7721 cells ($P < 0.05$) (Fig. 5B). Similarly, the western blot results showed that the hepatic γ-H2AX, DNA-PKc, and caspase-1 protein expression levels were significantly greater in the SMMC-7721 cells treated with RFA versus those not treated with RFA. Similar to the mRNA expression patterns, overexpression of AIM2 increased hepatic γ-H2AX and DNA-PKc protein expression levels. In contrast, knockdown of AIM2 suppressed the hepatic γ-H2AX and DNA-PKc protein levels in SMMC-7721 cells ($P < 0.05$) (Fig. 5C).

We next found that RFA treatment caused increased hepatic IL-1β and IL-18 mRNA expression levels in SMMC-7721 cells, as well as secreted protein levels in the cell culture supernatant ($P < 0.05$) (Fig. 6). Notably, SMMC-7721 cells with AIM2 overexpression exhibited dramatic increases in both hepatic IL-1β and IL-18 mRNA expression levels and protein secretion. In contrast, AIM2 knockdown in SMMC-7721 cells inhibited both hepatic IL-1β and IL-18 mRNA expression levels and protein secretion ($P < 0.05$) (Fig. 6). These results supported our hypothesis that AIM2 can exert a biological role in RFA-induced pyroptosis in HCC.

4. Discussion

The major novel findings of this study can be summarized as follows: (1) RFA treatment significantly inhibited tumor growth in BALB/c nude mice bearing HepG2 or SMMC-7721 cell-derived xenografts compared with the controls that did not receive RFA (Fig. 1); (2) RFA induced pyroptotic cell death of HepG2 or SMMC-7721 cells in the xenograft nude mice, as evidenced by significantly elevated expression levels of AIM2, NLRP3, caspase-1, γ-H2AX, and DNA-PKc in the liver tissues of the mice treated with RFA versus those of the controls (Fig. 2). Additionally, the serum levels IL-1β and IL-18 were significantly greater in the HepG2 or SMMC-7721 cell-derived xenograft mice treated with RFA compared with those not receiving RFA (Fig. 3). More pronounced effects were observed in the complete ablation group versus the partial ablation group of xenograft nude mice (Fig. 2–3); (3) Functional and mechanistic *in vitro* studies indicated that AIM2 exerts a direct role in RFA-induced pyroptosis. These findings were supported by experiments using knockdown or overexpression of AIM2 in SMMC-7721 cells (Fig. 4–6). Collectively, our results help elucidate the effects of RFA on the proliferation of hepatoma cells and induction of pyroptosis through AIM2-inflammasome signaling.

It has been well documented that hepatic inflammation is crucially involved in HCC development [8]. Over the last decade, there has been rapid progress in our understanding of inflammasome activation and its role in HCC pathogenesis, along with the complex interplay between inflammasome activation and other innate immune pathways (e.g., cyclic GMP-AMP synthase [cGAS]–stimulator of interferon genes [STING] signaling) [24]. For example, AIM2-like receptors are reportedly capable of inducing inflammasome activation, thereby further triggering caspases. Once activated, caspases can mediate the generation, maturation, and secretion of pro-inflammatory cytokines, mainly IL-1β and IL-18. As a result, excessive secretion of IL-1β and IL-18 can ultimately induce a form of programmed cell death referred to as pyroptosis [25–27], which can occur through canonical (caspase-1-dependent), non-canonical (caspase-4/5/11-dependent), and caspase-3-dependent pathways. Its key effectors, gasdermin proteins, form pores in the cell membrane that cause cell lysis and inflammatory cytokine release [28]; therefore, pyroptosis is closely linked to inflammation [29]. This relationship was experimentally confirmed in a mouse model, where NLRP3 inflammasome activation led to severe liver inflammation, hepatocyte pyroptosis, and fibrosis [30].

HBV and HCV infections are well-known causes of HCC. In fact, nearly 90% of HCC cases are associated with chronic hepatic inflammation [31,32]. Therefore, inflammasome-associated molecular mechanisms have been a major focus of HCC research. In the present study, we found that RFA treatment could induce pyroptosis in nude mice bearing HepG2 or SMMC-7721 cell-derived xenografts, as well as in SMMC-7721 cells *in vitro*. Our findings further supported that the AIM2-activated inflammasome could activate caspase-1, through which it enhanced the production and secretion of IL-1β and IL-18, then ultimately pyroptosis.

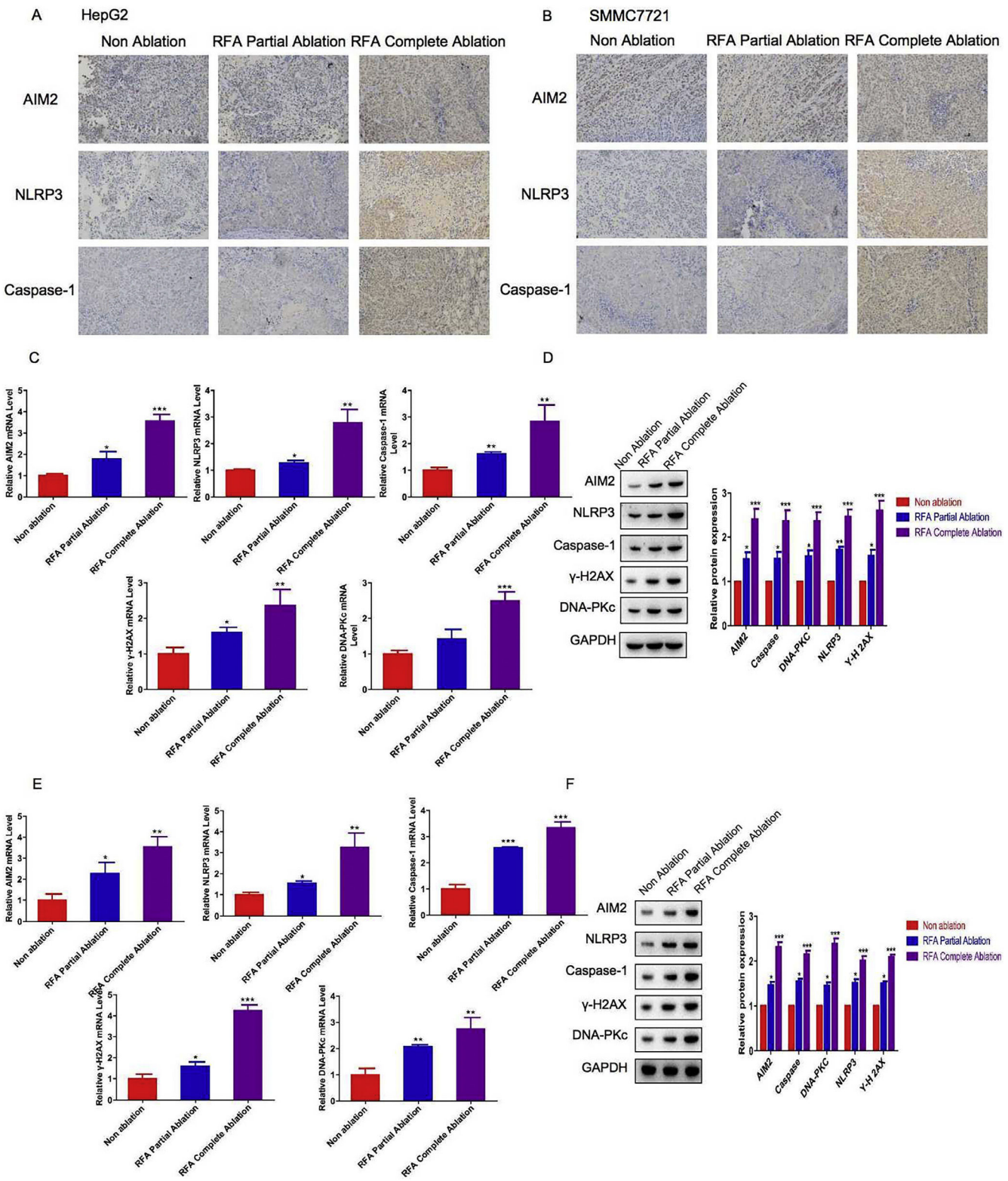

Fig. 2. Levels of inflammasome- and pyroptosis-related molecules with radiofrequency ablation (RFA) in xenograft mouse models. HepG2 and SMMC-7721 cell-derived xenograft nude mice were treated with RFA partial ablation, RFA complete ablation, or no ablation as a control (Non-ablation). After 4 weeks, the liver tissues were collected for subsequent analysis. Immunohistochemical analysis of inflammasome proteins before and after RFA in (A) HepG2 cell-derived xenograft nude mice and (B) SMMC-7721 cell-derived xenograft nude mice. Hepatic AIM2, NLRP3, caspase-1, γ-H2AX, and DNA-PKc (C) mRNA and (D) protein expression levels in HepG2 cell-derived xenograft nude mice. Hepatic AIM2, NLRP3, caspase-1, γ-H2AX, and DNA-PKc (E) mRNA and (F) protein expression levels in SMMC-7721 cell-derived xenograft nude mice. The hepatic AIM2, NLRP3, caspase-1, γ-H2AX, and DNA-PKc mRNA and protein expression levels were significantly greater in the HepG2 and SMMC-7721 cell-derived xenograft nude mice treated with RFA partial or complete ablation compared with the no-RFA ablation control mice. There were greater effects on these protein levels in the complete ablation group versus the partial ablation group. Data are presented as the mean ± SD. $^{*}P < 0.05$; $^{**}P < 0.01$; $^{***}P < 0.001$.

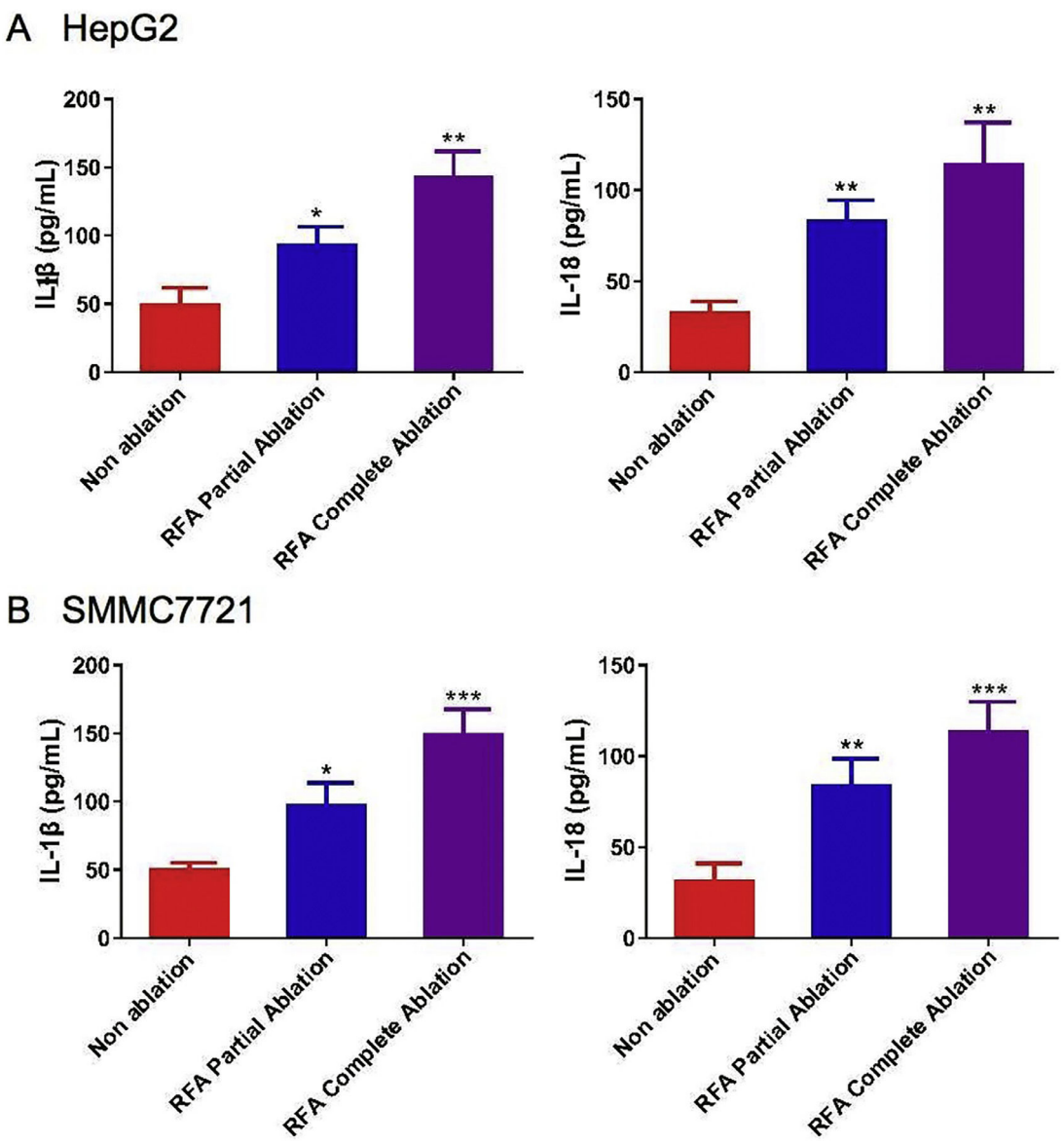

Fig. 3. Serum levels of interleukin (IL)-1β and IL-18 with radiofrequency ablation (RFA) in xenograft mouse models. The serum levels of IL-1β and IL-18 were examined by enzyme-linked immunosorbent assays (ELISAs) in (A) HepG2 cell-derived xenograft nude mice and (B) SMMC-7721 cell-derived xenograft nude mice after 4 weeks of RFA partial ablation, RFA complete ablation, or no ablation. Data are presented as the mean ± SD. $^{*}P < 0.05$; $^{**}P < 0.01$; $^{***}P < 0.001$.

Numerous previous studies have shown that the hepatic AIM2 levels are significantly reduced in HCC samples compared with matched histologically normal tissues from the same patients. Additionally, lower AIM2 expression levels are significantly correlated with more advanced HCC [20,21,33], as well as with poorer tumor differentiation and greater invasion and metastasis abilities. Overall, these observations suggest that the loss of AIM2 may contribute to HCC progression [20,21]. Moreover, Ma et al. showed that overexpressing AIM2 could significantly suppress tumor growth in a xenograft mouse model of HCC [20]. Furthermore, the potential role of AIM2 in HCC development has been recently investigated, with the results demonstrating that genetic silencing of AIM2 or caspase-1/11 could protect mice from the occurrence of HCC [34,35]. Our findings are consistent with these previous studies. To date, the exact roles of AIM2 and AIM2-activated inflammasomes in the action of RFA treatment for HCC have not been explored. Our results indicate that the inhibitory effects of RFA on the proliferation of hepatoma cells may involve the induction of pyroptosis through AIM2-inflammasome signaling. We postulated that exposure to RFA can cause cellular damage, triggering the release of self-DNA that can be sensed by AIM2 and other inflammasomes (e.g., cGAS), activating their respective pathways in the absence of infection and further enhancing inflammation.

Recent findings suggest that pyroptosis and IL-1β secretion, while usually coupled, can occur independently under certain conditions [36]. This uncoupling can contribute to prolonged inflammation or increased lethality, depending on the predominant process. In the present study, we observed both pyroptosis and cytokine release, suggesting a coupled response to RFA. Further investigation into the potential uncoupling of these processes in the context of RFA and HCC could provide additional mechanistic insights concerning inflammation and cell death.

Inflammasomes are multimolecular complexes with central roles in caspase-1 activation and pyroptosis induction [37]. In addition to their canonical functions, recent discoveries have revealed broader roles for inflammasomes in regulating various biological processes (e.g., eicosanoid storms, autophagy, and metabolism). These emerging functions highlight the multifaceted nature of inflammasomes and

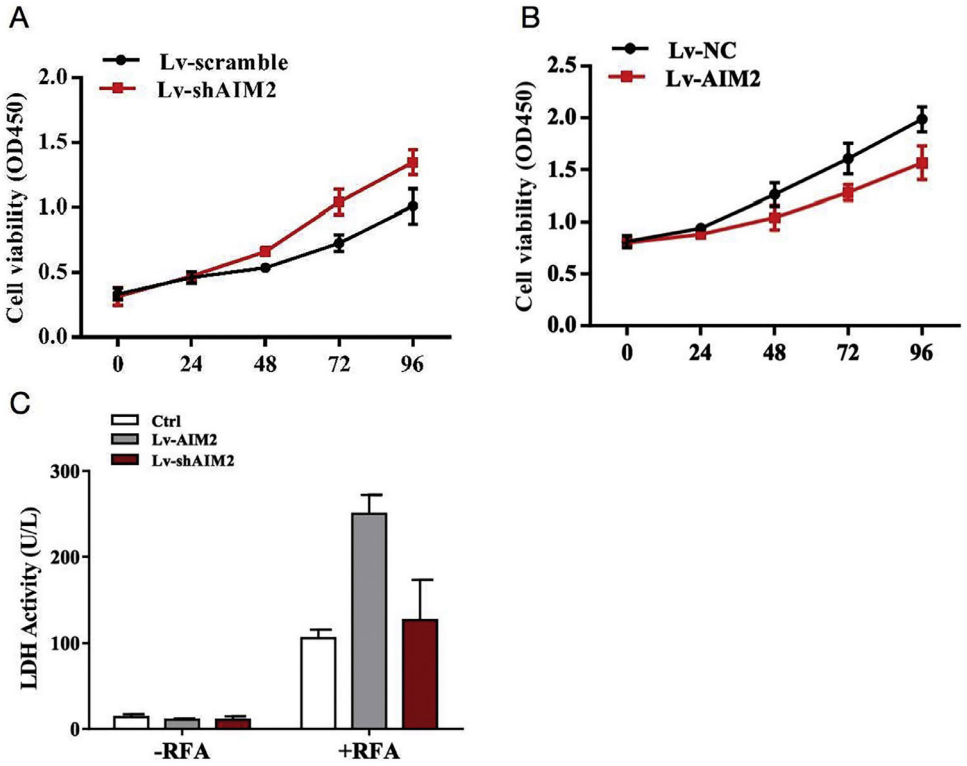

Fig. 4. Effects of AIM2 knockdown or overexpression on SMMC-7721 cell proliferation and lactate dehydrogenase (LDH) release. Proliferation assays showed the effects of (A) knockdown or (B) overexpression of AIM2 on SMMC-7721 cell viability. Knocking down AIM2 expression with an AIM2-specific short hairpin RNA (shRNA) (shAIM2) enhanced the proliferation of SMMC-7721 cells compared with the scrambled shRNA control. By contrast, overexpression of AIM2 with an expression vector (OS-AIM2) attenuated the proliferation of SMMC-7721 cells compared with the negative control (NC). (C) An LDH release assay revealed the effects of AIM2 knockdown or overexpression on LDH release in SMMC-7721 cells with or without exposure to RFA. Data are presented as the mean ± SD. $P < 0.05$ indicated a significant difference between groups.

their potential as therapeutic targets in various diseases. Here, we focused on canonical functions of the AIM2 inflammasome in mediating pyroptosis and cytokine release in response to RFA. Future studies exploring the non-canonical functions of AIM2 and other inflammasomes in the context of HCC could provide a more comprehensive understanding of their roles in tumor biology and treatment responses.

The regulation of inflammasome activity is a complex process involving multiple mechanisms [38]. Positive regulation can occur through transcriptional upregulation of inflammasome components and post-translational modifications (e.g., ubiquitination and phosphorylation). Negative regulation can be mediated by microRNAs, inhibitory proteins, and cellular processes such as autophagy. In our study, we observed increased expression of AIM2 and NLRP3 in RFA-treated xenograft mice, suggesting a role for transcriptional regulation in the activation of these inflammasomes. Future studies could explore post-translational modifications and negative regulatory mechanisms that modulate AIM2 and NLRP3 activities in the context of RFA and HCC.

The long-term outcomes and prognostic factors for RFA in HCC have been investigated [39]. In a study of 1,170 primary HCC patients, RFA achieved complete tumor ablation in 99.4% of treatments, with 5-year and 10-year survival rates of 60.2% and 27.3%, respectively. Thus, RFA constitutes a potentially curative treatment for HCC, capable of achieving long-term survival. Despite the high local control rates, distant recurrences remained frequent (5-year and 10-year rates of 74.8% and 80.8%, respectively). These findings highlight the importance of understanding the molecular mechanisms that underlie the effects of RFA, as well as the need for combinatorial approaches to prevent recurrence.

In recent years, immune-based treatments have emerged as promising strategies for HCC [40]. Considering the chronic inflammation associated with HCC, immunotherapy represents an attractive approach to harness the immune system for disease control. Various immune-based strategies are in development; there is particular interest in the combination of immunotherapy with standard treatments (e.g., RFA). Combinatorial approaches have shown potential in small studies; further research is needed to optimize these strategies and inform patient selection.

Despite advancements in HCC research, it remains challenging to translate preclinical findings into clinical applications. The so-called "valley of death" between basic research and clinical translation is characterized by high attrition rates, irreproducible data, and limited clinical impact [41]. Confirmatory multicenter studies can enhance the robustness and translatability of preclinical evidence before clinical trials begin [42]. The successful development of the B-cell lymphoma 2 (BCL2) inhibitor venetoclax provides a compelling example of how preclinical research can guide clinical development [43]. Extensive preclinical studies regarding apoptosis and BCL2 biology informed the design and optimization of venetoclax, leading to clinical success in the treatment of hematologic malignancies. Similarly, clinical studies are necessary to validate the translatability of our findings.

This study has some potential limitations. First, we found that AIM2 expression levels were markedly elevated in response to RFA in the mice bearing HepG2 or SMMC-7721 cell-derived xenografts, as well as in cell culture. However, the molecular pathways through which AIM2 is upregulated remain unknown. We propose that, in the absence of infection caused by pathogens, AIM2 may sense RFA-associated DNA, assemble and activate the inflammasome complex, then promote the secretion of pro-inflammatory cytokines that thus induce pyroptosis. Given that compelling evidence of the actions of AIM2 beyond the inflammasome complex has been reported [44–49], it would be interesting to explore whether AIM2 can play an

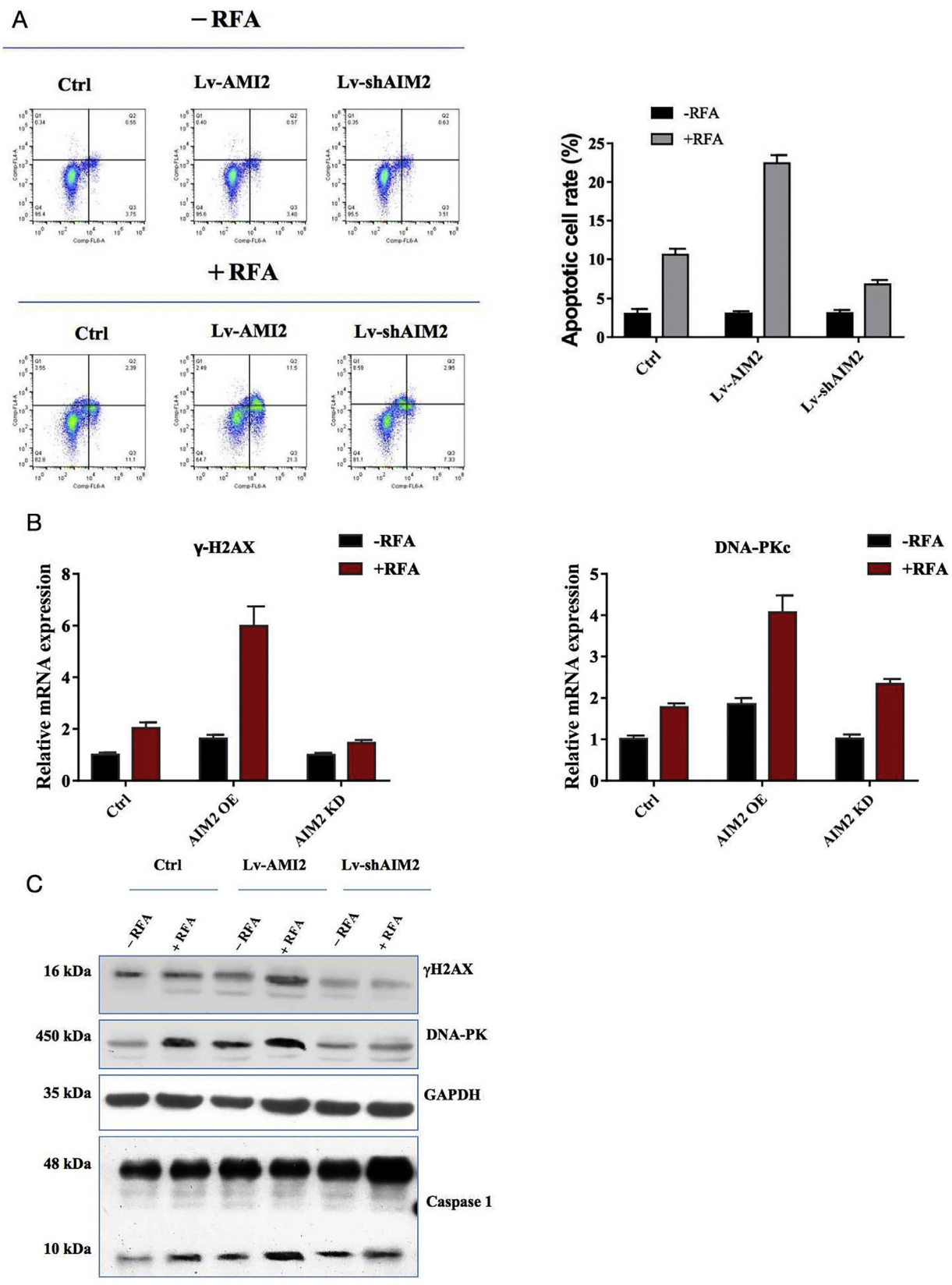

Fig. 5. Effects of AIM2 knockdown or overexpression on radiofrequency ablation (RFA)-induced pyroptosis in SMMC-7721 cells. (A) Effects of AIM2 overexpression or knockdown on RFA-induced pyroptosis. Pyroptosis was determined by flow cytometry. Overexpression of AIM2 with an expression vector (OS-AIM2) induced the pyroptosis of SMMC-7721 cells compared with the negative control (NC). By contrast, knockdown of AIM2 with an AIM2-specific short hairpin RNA (shRNA) (shAIM) inhibited the pyroptosis of SMMC-7721 cells compared with the scrambled shRNA control. (B) The effects of AIM2 overexpression or knockdown on the mRNA levels of pyroptosis-related molecules before and after RFA were examined in SMMC-7721 cells using qRT-PCR assays. (C) Western blot analysis of the effects of AIM2 overexpression or knockdown on the protein levels of pyroptosis-related molecules before and after RFA in SMMC-7721 cells. $P < 0.05$ indicated a significant difference between groups.

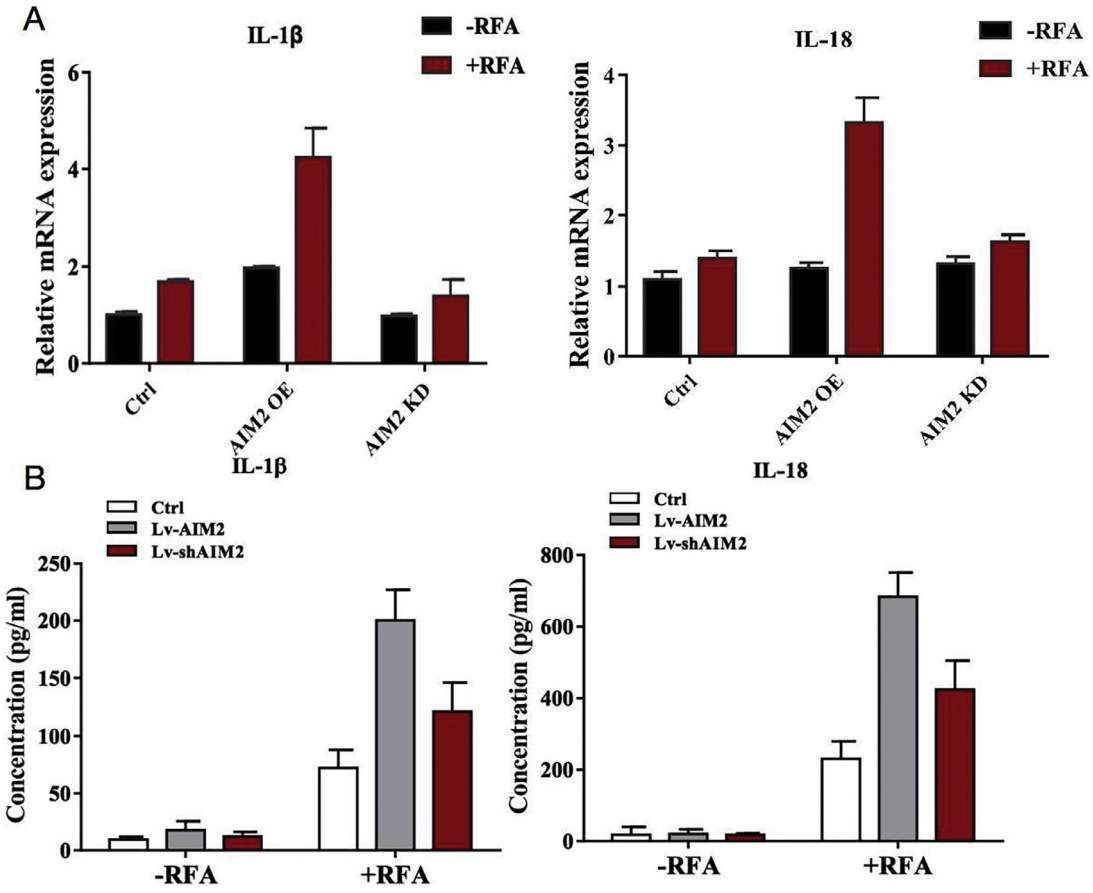

Fig. 6. Effects of AIM2 knockdown or overexpression on pro-inflammatory cytokine production by SMMC-7721 cells. AIM2 was overexpressed in SMMC-7721 cells using an expression vector (OS-AIM2). AIM2 was knocked down in SMMC-7721 cells using short hairpin RNAs (shRNAs). (A) qRT-PCR analysis was conducted to measure the mRNA expression levels of interleukin (IL)-1β and IL-18. (B) Enzyme-linked immunosorbent assays (ELISAs) were performed to determine the IL-1β and IL-18 levels in the cell culture supernatant of SMMC-7721 cells. $P < 0.05$ indicated a significant difference between groups.

inflammasome-independent role in HCC and RFA treatment. Further in-depth investigations of the underlying molecular mechanisms are currently underway in our laboratory. Second, we utilized LDH measurements to assess both cell death and proliferation. More targeted markers, such as proliferating cell nuclear antigen (PCNA; highly expressed during DNA synthesis [50]) and Ki-67 antigen (present during all active phases of the cell cycle [51,52]), could be used to specifically evaluate cell proliferation. Future analyses involving these markers would enable more direct assessment of proliferative activity in HCC cells. Finally, this exploratory analysis used small sample sizes based on standard laboratory practices and ethical considerations; additional studies with larger sample sizes and detailed power analyses are needed to confirm our findings.

5. Conclusions

Taken together, we found that RFA treatment could suppress tumor growth and induce pyroptosis in *in vitro* and *in vivo* models of HCC. In addition, we identified AIM2-mediated activation of inflammasome signaling as an important cell death mechanism. Therefore, these findings advance our understanding of the biological function of AIM2. Therapeutic intervention with AIM2-mediated inflammasome signaling may help improve RFA treatment outcomes for HCC patients.

Funding

This study was supported by the Youth Project of Changzhou Health Commission (grant number QN202341), the Natural Science Foundation of Jiangsu Province (grant number BK20180185), China Postdoctoral Science Foundation (grant number 2020M681447), and Postdoctoral Science Foundation of Jiangsu Province (grant number 20202175).

Authors' contributions

FH and CW conceived and designed the study. ZH contributed significantly to data analysis and manuscript preparation. CW and FH performed the data analyses and wrote the manuscript.

Data availability

The datasets used and/or analyzed during the current study are available from the corresponding author upon reasonable request.

Conflicts of interest

None.

Acknowledgements

We thank J. Iacona, Ph.D., and Ryan Chastain-Gross, Ph.D., from Liwen Bianji (Edanz) (www.liwenbianji.cn) for editing the English text of a draft of this manuscript.

References

[1] Yang JD, Hainaut P, Gores GJ, Amadou A, Plymoth A, Roberts LR. A global view of hepatocellular carcinoma: trends, risk, prevention and management. Nat Rev Gastroenterol Hepatol 2019;16:589–604. https://doi.org/10.1038/s41575-019-0186-y.

[2] Toh MR, Wong EYT, Wong SH, Ng AWT, Loo LH, Chow PK, Ngeow J. Global epidemiology and genetics of hepatocellular carcinoma. Gastroenterology 2023;164:766–82. https://doi.org/10.1053/j.gastro.2023.01.033.

[3] Llovet JM, Villanueva A, Lachenmayer A, Finn RS. Advances in targeted therapies for hepatocellular carcinoma in the genomic era. Nat Rev Clin Oncol 2015;12:408–24. https://doi.org/10.1038/nrclinonc.2015.103.

[4] Llovet JM, Kelley RK, Villanueva A, Singal AG, Pikarsky E, Roayaie S, et al. Hepatocellular carcinoma. Nat Rev Dis Primers 2021;7:6. https://doi.org/10.1038/s41572-020-00240-3.

[5] Chen W, Zheng R, Baade PD, Zhang S, Zeng H, Bray F, et al. Cancer statistics in China. CA Cancer J Clin 2016;66:115–32. https://doi.org/10.3322/caac.21338.

[6] Akinyemiju T, Abera S, Ahmed M, Alam N, Alemayohu MA, Allen C, et al. The burden of primary liver cancer and underlying etiologies from 1990 to 2015 at the global, regional, and national level: Results from the global burden of disease study. JAMA Oncol 2017;3:1683–91. https://doi.org/10.1001/jamaoncol.2017.3055.

[7] Szabo G, Petrasek J. Inflammasome activation and function in liver disease. Nat Rev Gastroenterol Hepatol 2015;12:387–400. https://doi.org/10.1038/nrgastro.2015.94.

[8] Galun E. Liver inflammation and cancer: the role of tissue microenvironment in generating the tumor-promoting niche (TPN) in the development of hepatocellular carcinoma. Hepatology 2016;63:354–6. https://doi.org/10.1002/hep.28344.

[9] Man SM. Inflammasomes in the gastrointestinal tract: infection, cancer and gut microbiota homeostasis. Nat Rev Gastroenterol Hepatol 2018;15:721–37. https://doi.org/10.1038/s41575-018-0054-1.

[10] Luan J, Ju D. Inflammasome: A double-edged sword in liver diseases. Front Immunol 2018;9:2201. https://doi.org/10.3389/fimmu.2018.02201.

[11] Izzo F, Granata V, Grassi R, Fusco R, Palaia R, Delrio P, et al. Radiofrequency Ablation and Microwave Ablation in Liver Tumors: An Update. Oncologist 2019;24:e990–e1005. https://doi.org/10.1634/theoncologist.2018-0337.

[12] Lugrin J, Martinon F. The AIM2 inflammasome: Sensor of pathogens and cellular perturbations. Immunol Rev 2018;281:99–114. https://doi.org/10.1111/imr.12618.

[13] Wang B, Yin Q. AIM2 inflammasome activation and regulation: A structural perspective. J Struct Biol 2017;200:279–82. https://doi.org/10.1016/j.jsb.2017.08.001.

[14] Jin T, Perry A, Jiang J, Smith P, Curry JA, Unterholzner L, et al. Structures of the HIN domain:DNA complexes reveal ligand binding and activation mechanisms of the AIM2 inflammasome and IFI16 receptor. Immunity 2012;36:561–71. https://doi.org/10.1016/j.immuni.2012.02.014.

[15] Morrone SR, Matyszewski M, Yu X, Delannoy M, Egelman E, Sohn J. Assembly-driven activation of the AIM2 foreign-dsDNA sensor provides a polymerization template for downstream ASC. Nat Commun 2015;6:7827. https://doi.org/10.1038/ncomms8827.

[16] Fernandes-Alnemri T, Yu JW, Datta P, Wu J, Alnemri ES. AIM2 activates the inflammasome and cell death in response to cytoplasmic DNA. Nature 2009;458:509–13. https://doi.org/10.1038/nature07710.

[17] Hornung V, Ablasser A, Charrel-Dennis M, Bauernfeind F, Horvath G, Caffrey DR, et al. AIM2 recognizes cytosolic dsDNA and forms a caspase-1-activating inflammasome with ASC. Nature 2009;458:514–8. https://doi.org/10.1038/nature07725.

[18] Zheng P, Xiao W, Zhang J, Zheng X, Jiang J. The role of AIM2 in human hepatocellular carcinoma and its clinical significance. Pathol Res Pract 2023;245:154454. https://doi.org/10.1016/j.prp.2023.154454.

[19] Lozano-Ruiz B, González-Navajas JM. The emerging relevance of AIM2 in liver disease. Int J Mol Sci 2020;21:6535. https://doi.org/10.3390/ijms21186535.

[20] Ma X, Guo P, Qiu Y, Mu K, Zhu L, Zhao W, et al. Loss of AIM2 expression promotes hepatocarcinoma progression through activation of mTOR-S6K1 pathway. Oncotarget 2016;7:36185–97. https://doi.org/10.18632/oncotarget.9154.

[21] Chen SL, Liu LL, Lu SX, Luo RZ, Wang CH, Wang H, et al. HBx-mediated decrease of AIM2 contributes to hepatocellular carcinoma metastasis. Mol Oncol 2017;11:1225–40. https://doi.org/10.1002/1878-0261.12090.

[22] Alzahri MS, Mousa SA, Almomen AM, Hasanato RM, Polimeni JM, Racz MJ. Lactate dehydrogenase as a biomarker for early renal damage in patients with sickle cell disease. Saudi J Kidney Dis Transpl 2015;26:1161–8. https://doi.org/10.4103/1319-2442.168596.

[23] Forkasiewicz A, Dorociak M, Stach K, Szelachowski P, Tabola R, Augoff K. The usefulness of lactate dehydrogenase measurements in current oncological practice. Cell Mol Biol Lett 2020;25:35. https://doi.org/10.1186/s11658-020-00228-7.

[24] Liu J, Zhou J, Luan Y, Li X, Meng X, Liao W, et al. cGAS-STING, inflammasomes and pyroptosis: an overview of crosstalk mechanism of activation and regulation. Cell Commun Signal 2024;22:22. https://doi.org/10.1186/s12964-023-01466-w.

[25] Martinon F, Burns K, Tschopp J. The inflammasome: a molecular platform triggering activation of inflammatory caspases and processing of proIL-beta. Mol Cell 2002;10:417–26. https://doi.org/10.1016/s1097-2765(02)00599-3.

[26] Kayagaki N, Wong MT, Stowe IB, Ramani SR, Gonzalez LC, Akashi-Takamura S, et al. Noncanonical inflammasome activation by intracellular LPS independent of TLR4. Science 2013;341:1246–9. https://doi.org/10.1126/science.1240248.

[27] Liu X, Zhang Z, Ruan J, Pan Y, Magupalli VG, Wu H, et al. Inflammasome-activated gasdermin D causes pyroptosis by forming membrane pores. Nature 2016;535:153–8. https://doi.org/10.1038/nature18629.

[28] Shi J, Zhao Y, Wang K, Shi X, Wang Y, Huang H, et al. Cleavage of GSDMD by inflammatory caspases determines pyroptotic cell death. Nature 2015;526:660–5. https://doi.org/10.1038/nature15514.

[29] Chai R, Li Y, Shui L, Ni L, Zhang A. The role of pyroptosis in inflammatory diseases. Front Cell Dev Biol 2023;11:1173235. https://doi.org/10.3389/fcell.2023.1173235.

[30] Wree A, Eguchi A, McGeough MD, Pena CA, Johnson CD, Canbay A, et al. NLRP3 inflammasome activation results in hepatocyte pyroptosis, liver inflammation, and fibrosis in mice. Hepatology 2014;59:898–910. https://doi.org/10.1002/hep.26592.

[31] Llovet JM, Zucman-Rossi J, Pikarsky E, Sangro B, Schwartz M, Sherman M, et al. Hepatocellular carcinoma. Nat Rev Dis Primers 2016;2:16018. https://doi.org/10.1038/nrdp.2016.18.

[32] Ringelhan M, Pfister D, O'Connor T, Pikarsky E, Heikenwalder M. The immunology of hepatocellular carcinoma. Nat Immunol 2018;19:222–32. https://doi.org/10.1038/s41590-018-0044-z.

[33] Sonohara F, Inokawa Y, Kanda M, Nishikawa Y, Yamada S, Fujii T, et al. Association of inflammasome components in background liver with poor prognosis after curatively-resected hepatocellular carcinoma. Anticancer Res 2017;37:293–300. https://doi.org/10.21873/anticanres.11320.

[34] Martínez-Cardona C, Lozano-Ruiz B, Bachiller V, Peiró G, Algaba-Chueca F, Gómez-Hurtado I, et al. AIM2 deficiency reduces the development of hepatocellular carcinoma in mice. Int J Cancer 2018;143:2997–3007. https://doi.org/10.1002/ijc.31827.

[35] Macek Jilkova Z, Kurma K, Decaens T. Animal models of hepatocellular carcinoma: The role of immune system and tumor microenvironment. Cancers (Basel) 2019;11:1478. https://doi.org/10.3390/cancers11101487.

[36] Li Y, Jiang Q. Uncoupled pyroptosis and IL-1β secretion downstream of inflammasome signaling. Front Immunol 2023;14:1128358. https://doi.org/10.3389/fimmu.2023.1128358.

[37] Rathinam VA, Fitzgerald KA. Inflammasome complexes: emerging mechanisms and effector functions. Cell 2016;165:792–800. https://doi.org/10.1016/j.cell.2016.03.046.

[38] Latz E, Xiao TS, Stutz A. Activation and regulation of the inflammasomes. Nat Rev Immunol 2013;13:397–411. https://doi.org/10.1038/nri3452.

[39] Shiina S, Tateishi R, Arano T, Uchino K, Enooku K, Nakagawa H, et al. Radiofrequency ablation for hepatocellular carcinoma: 10-year outcome and prognostic factors. Am J Gastroenterol 2012;107:569–77 quiz 578. https://doi.org/10.1038/ajg.2011.425.

[40] Greten TF, Wang XW, Korangy F. Current concepts of immune based treatments for patients with HCC: from basic science to novel treatment approaches. Gut 2015;64:842–8. https://doi.org/10.1136/gutjnl-2014-307990.

[41] Seyhan AA. Lost in translation: the valley of death across preclinical and clinical divide – identification of problems and overcoming obstacles. Transl Med Commun 2019;4:18. https://doi.org/10.1186/s41231-019-0050-7.

[42] Drude NI, Martinez-Gamboa L, Danziger M, Collazo A, Kniffert S, Wiebach J, et al. Planning preclinical confirmatory multicenter trials to strengthen translation from basic to clinical research – a multi-stakeholder workshop report. Transl Med Commun 2022;7:24. https://doi.org/10.1186/s41231-022-00130-8.

[43] Leverson JD, Sampath D, Souers AJ, Rosenberg SH, Fairbrother WJ, Amiot M, et al. Found in translation: how preclinical research is guiding the clinical development of the BCL2-selective inhibitor venetoclax. Cancer Discov 2017;7:1376–93. https://doi.org/10.1158/2159-8290.CD-17-0797.

[44] El-Zaatari M, Bishu S, Zhang M, Grasberger H, Hou G, Haley H, et al. Aim2-mediated/IFN-β-independent regulation of gastric metaplastic lesions via CD8+ T cells. JCI Insight 2020;5:e94035. https://doi.org/10.1172/jci.insight.94035.

[45] Furrer A, Hottiger MO, Valaperti A. Absent in Melanoma 2 (AIM2) limits pro-inflammatory cytokine transcription in cardiomyocytes by inhibiting STAT1 phosphorylation. Mol Immunol 2016;74:47–58. https://doi.org/10.1016/j.molimm.2016.04.009.46.

[46] Farshchian M, Nissinen L, Siljamäki E, Riihilä P, Piipponen M, Kivisaari A, et al. Tumor cell-specific AIM2 regulates growth and invasion of cutaneous squamous cell carcinoma. Oncotarget 2017;8:45825–36. https://doi.org/10.18632/oncotarget.17573.

[47] Man SM, Zhu Q, Zhu L, Liu Z, Karki R, Malik A, et al. Critical Role for the DNA Sensor AIM2 in Stem Cell Proliferation and Cancer. Cell 2015;162:45–58. https://doi.org/10.1016/j.cell.2015.06.001.

[48] Wilson JE, Petrucelli AS, Chen L, Koblansky AA, Truax AD, Oyama Y, et al. Inflammasome-independent role of AIM2 in suppressing colon tumorigenesis via DNA-PK and Akt. Nat Med 2015;21:906–13. https://doi.org/10.1038/nm.3908.

[49] Qi M, Dai D, Liu J, Li Z, Liang P, Wang Y, et al. AIM2 promotes the development of non-small cell lung cancer by modulating mitochondrial dynamics. Oncogene 2020;39:2707–23. https://doi.org/10.1038/s41388-020-1176-9.

[50] Celis JE, Celis A. Cell cycle-dependent variations in the distribution of the nuclear protein cyclin proliferating cell nuclear antigen in cultured cells: subdivision of S phase. Proc Natl Acad Sci U S A 1985;82:3262–6. https://doi.org/10.1073/pnas.82.10.3262.

[51] Scholzen T, Gerdes J. The Ki-67 protein: from the known and the unknown. J Cell Physiol 2000;182:311–22. https://doi.org/10.1002/(SICI)1097-4652(200003)182:3<311::AID-JCP1>3.0.CO;2-9.

[52] Ligasová A, Koberna K. DNA dyes-highly sensitive reporters of cell quantification: comparison with other cell quantification methods. Molecules 2021;26:5515. https://doi.org/10.3390/molecules26185515.